JVST A
Journal of Vacuum Science & Technology A

Continuous-wave laser doping of micrometer-sized features in gallium arsenide using a dimethylzinc ambient

Cite as: Journal of Vacuum Science & Technology A **8**, 1618 (1990); https://doi.org/10.1116/1.576775
Submitted: 25 October 1989 • Accepted: 27 December 1989 • Published Online: 04 June 1998

T. J. Licata, D. V. Podlesnik, H. Tang, et al.

Journal of Vacuum Science & Technology A **8**, 1618 (1990); https://doi.org/10.1116/1.576775 **8**, 1618

Continuous-wave laser doping of micrometer-sized features in gallium arsenide using a dimethylzinc ambient

T. J. Licata, D. V. Podlesnik, H. Tang, I. P. Herman, and R. M. Osgood, Jr.
Microelectronics Sciences Laboratories, Columbia University, New York, New York 10027

S. A. Schwarz
Bell Communications Research, Red Bank, New Jersey 07701

(Received 25 October 1989; accepted 27 December 1989)

We present a single-step process for the direct writing of micron-scale Zn-doped regions on GaAs substrates. A focused continuous-wave Ar^+ laser drives both pyrolysis of the dimethylzinc source gas and solid-state diffusion of the Zn atoms into the GaAs. Secondary ion mass spectroscopy (SIMS) has been used to measure the dopant depth profiles as a function of laser-induced temperature. Raman microprobe spectroscopy has been used to corroborate the SIMS measurements and measure the lateral extent of micron-sized doped lines. In a preliminary measurement of electrical activation, Al contacts to *n*-GaAs have been modified using the process.

I. INTRODUCTION

The doping of semiconducting materials is a basic step in the fabrication of electronic and optoelectronic devices. The conventional techniques for fabricating doped regions require several photolithographic steps followed by thermal diffusion or ion implantation. Recently, several laser or ion focused-beam doping techniques have been investigated to provide the ability to vary doping levels across a wafer or within a device. While the use of focused ion beams provides the ability to grade doping patterns horizontally within a single device,[1] localized implantation requires subsequent high-temperature processing of the entire wafer to activate the dopant and anneal out the ion-induced damage. Further, the need for a high-temperature post-implant anneal makes it difficult to form shallow, highly doped, near-surface regions.

Ideally, a continuous-wave (cw) laser-based process for the writing of device-sized doped features addresses these concerns in that it provides for three-dimensional control of dopant distribution in a truly local fashion. This is achieved by control over any two of the three parameters: laser power, dwell time, and source atom availability. While possible dopant sources include spin-on sources and doped glassy layers, real time control over source atom availability can be achieved only through use of a gas-phase delivery system. An added benefit to gas-phase doping is its potential compatibility with *in situ* metalorganic molecular-beam epitaxy (MOMBE) and metalorganic chemical vapor deposition (MOCVD) processing.

There have been several previous successful implementations of laser doping. For example, Ehrlich, Osgood, and Deutsch have used etching and electrical characterization to document a two-beam, UV-visible approach to writing Cd-doped regions in InP.[2] Similarly, Tsao and Ehrlich's work on laser-diffused boron and phosphorus in silicon demonstrated that laser doping could produce doped regions significantly narrower than the laser-beam width, due to the nonlinear dependence of diffusion rate on temperature.[3] Finally, Nissim, Gibbons, and Gold have used electrical characterization to show that nonalloyed ohmic contacts can be made to *n*-GaAs by laser doping Sn from a spin-on SnO_2/SiO_2 film.[4]

Here, we report on the application of a visible cw laser to the direct writing of shallow doped regions in GaAs using a dimethylzinc (DMZn) ambient. In these experiments, a focused 514 nm cw laser beam is used to induce a spatially confined, well-controlled temperature rise on the GaAs surface. The Zn dopant is carried to the surface via gas-phase DMZn molecules, which pyrolytically dissociate on the heated surface at temperatures above 250 °C,[5] thereby establishing a population of Zn atoms in contact with the heated surface. At the moderate homologous temperatures employed here $[T/T_{\mathrm{melt}}(\mathrm{GaAs}) \approx 1/2]$, some fraction of the Zn atoms are incorporated into the lattice as dopant through solid-state diffusion.

It is well known that at elevated temperatures, i.e., ~650 °C, near-surface As depletion of GaAs occurs with a corresponding degradation of its electrical properties. In addition, the exposure of GaAs to pure Zn at typical doping temperatures can cause surface degradation by dissolution of the GaAs.[6] Accordingly, it is particularly important to establish the process parameter window for damage-free doping.

II. EXPERIMENTAL APPARATUS

In all the experiments detailed here, the 514 nm beam from an Ar^+ laser is focused on the surface of a GaAs sample mounted in a diffusion-pumped stainless-steel cell having a base pressure of 5×10^{-7} Torr. The laser beam is focused through a quartz window to a 2.5 μm spot on the sample surface using a 10X microscope objective (N.A. = 0.2). The cell can be filled statically or dynamically with 0.01–1000 Torr, as measured by capacitance manometers, and is moved beneath the stationary beam by computer-controlled stages having a 0.25 μm minimum step size. The desired writing pattern can be programmed into the computer and executed

0734-2101/90/031618-05$01.00

at a single speed selected from those available to the stages (0.1–40 μm/s).

All GaAs samples were cleaned by degreasing using 10 min sequential immersions in trichloroethylene, acetone, and methanol. A relatively oxide-free surface was obtained by rinsing the freshly degreased sample in DI H_2O followed by a 2 min rinse in 50% NH_4OH, 50% DI H_2O. The samples were blow dried in dry N_2 and loaded into the high-vacuum cell within 2 min. The cell and bellows exposed to air during sample loading were baked for 12 h at 100 °C, yielding a base pressure in the high 10^{-7} Torr range as measured upstream from the cell and flow controllers using an ion gauge.

We have used several analytical techniques to investigate the doping process. First, optical microscopy, scanning electron microscopy (SEM), stylus profilometry, and reflected laser intensity analysis were used to assess any damage to the GaAs caused by laser irradiation. Second, secondary ion mass spectroscopy (SIMS) has been employed to observe directly the presence of high concentrations of laser-diffused Zn atoms in the near-surface region of GaAs substrates, as well as to determine the dependence of the doping process on laser-induced temperature. Raman spectroscopy has been employed to corroborate the doping found using SIMS and to investigate the lateral resolution of the process. Third, preliminary evaluation of the electrical activation of the Zn dopant has been obtained by modifying Al–GaAs contacts using the laser-doping process.

III. TEMPERATURE CALCULATIONS

Due to the difficulties involved with direct measurement of temperature on the micrometer scale, laser-induced temperatures during the doping process were based on numerical calculations of the temperature distribution in three dimensions. Specifically, we used Lax's solution of the nonlinear heat conduction equation for the case of nonlinear, temperature-dependent thermal conductivity.[7] The thermal conductivities[8] were fitted to the $1/T$ dependence appropriate for each of the background doping levels in the GaAs substrates. Since experimental data on temperature-dependent thermal conductivities are not available for GaAs for temperatures above ~650 °C, the thermal conductivity curve was extrapolated up to the melting point (1238 °C), taking into account the effect of radiative transport within the crystal at high temperature.[9] A temperature-independent reflectivity of 0.375 was used for the 514 nm beam.[10]

For calculation of laser-induced temperature, the focused spot size was measured by scanning, in two orthogonal directions, a cleaved silicon wafer edge beneath the focused beam. The incident laser power was controlled through a range from 1 to 160 mW using a quartz-plate variable optical density attenuator. For the typical focused beam width of 2.5 μm (full width between $1/e$ intensity points), these values correspond to laser power densities of 20–3300 kW/cm², allowing the temperature rise at the GaAs surface to be varied up to the melting point. Finally, we note that the laser-induced temperatures due to cw irradiation reach their steady-state values on a far shorter time scale ($\sim 10^{-6}$ s)[11] than the dwell times used in our experiments (0.1 s). Thus, our calculated temperatures are independent of the scan speeds employed here.

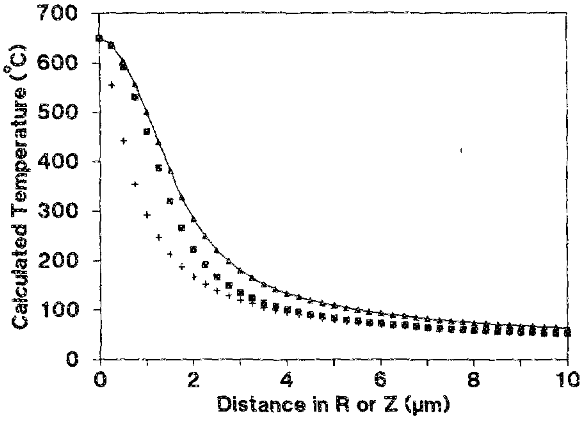

FIG. 1. Calculated (Ref. 7) temperature profiles in depth and radially from the center of a 514 nm beam focused to 2.5 μm onto $5\times10^{16}/cm^3$ *n*-doped GaAs. *R*:514 nm (■), *R*:799 nm (—), *Z*:514 nm (+), *Z*:799 nm (▲).

Figure 1 shows the temperature distribution away from the center of the focused spot radially (R) and into the substrate (Z) for laser beams of two different wavelengths focused to a width of 2.5 μm on $5\times10^{16}/cm^3$ *n*-GaAs, with incident powers chosen to yield a peak temperature of 650 °C. For the 514 nm beam used in our experiments, the short absorption length ($1/\alpha$) of ~1080 Å[12] results in a temperature distribution that falls off more rapidly in depth than radially. To increase the aspect ratio of the temperature profile (depth/radius) for a given spot size, a more penetrating wavelength can be used. For example, Fig. 1 also shows the temperature distribution in R and Z for 799 nm radiation from a Kr^+ laser (which was not used in our doping experiments). A reflectivity of 0.325 was used for this calculation.[10] In this case, the absorption depth in GaAs is ~7390 Å[12] and the temperature profiles in R and Z are almost identical. Hence, for a given final doping depth, greater lateral resolution would be expected for the 799 nm beam than for the 514 nm beam. On the other hand, for a given induced temperature, the 514 nm beam will result in better control over ultimate dopant depth.

IV. EXPERIMENTAL RESULTS

In order to demonstrate laser doping, GaAs samples were illuminated at various incident powers focused to 2.5 μm. The incident powers were chosen to raise the temperature within the focused spot to 500–650 °C, i.e., temperatures high enough to allow solid-state diffusion to occur. A pressure of 0.01 Torr of DMZn and a scan speed of 25 μm/s were used based on the process window considerations to be detailed below. No Zn deposit was visible on the surface after processing. We believe that during laser irradiation, most of the Zn atoms that do not diffuse into the GaAs desorb from the surface. Desorption of Zn from GaAs substrates has been noted previously at temperatures of 330 °C and above.[13] Nevertheless, all processed samples were dipped in 10% HCl for 1 min to eliminate the possibility of a thin film of Zn

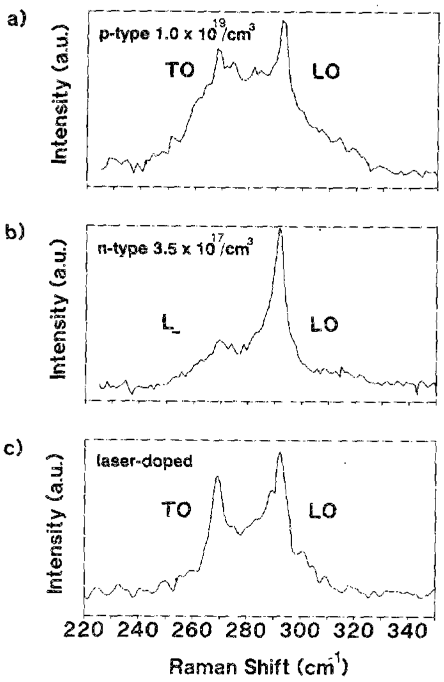

FIG. 2. Typical Raman spectra observed for unprocessed GaAs with (a) Zn doping and (b) Si doping. (c) The spectrum for an n-type surface transformed to p-type by laser doping.

atoms affecting subsequent measurements.

Raman microprobe spectroscopy was used to ascertain the presence of doping atoms and their lateral extent. This noninvasive technique is particularly useful because it provides mapping of doped regions with micron-scale lateral resolution. Furthermore, the probe samples only a near-surface region of the GaAs corresponding to half the absorption depth of the probing radiation. This depth is well matched to the depth of our laser-doped regions.

Near-surface regions of GaAs have been extensively studied by this technique previously.[14] It has been shown that for a given scattering configuration, the positions and intensities of observed Raman peaks vary with sample doping in a well characterized and understood manner. When free electrons from n-type doping are present ($n \geqslant 10^{17}/\mathrm{cm}^3$), plasmons couple with the longitudinal optical (LO) mode to yield the L_- peak near 270 cm^{-1} and weaker, broader L_+ peak at > 300 cm^{-1}, which bracket the LO peak at 292 cm^{-1}. However, when free holes are present, the coupling of collective hole excitations to the LO mode is inconsequential and the L_- and L_+ peaks are not observed.[15] Instead, p-type material exhibits the impurity-induced transverse optical (TO) mode at 268 cm^{-1}, which is forbidden in undoped (100) GaAs in backscattering geometry.[16] This characteristic behavior is seen in Figs. 2(a) and 2(b), which shows Raman spectra for unprocessed Zn-doped p- and Si-doped n-type materials.

In the Raman experiment, n-type $3.5\times10^{17}/\mathrm{cm}^3$ Si-doped substrates were adopted so that a transformation of the near-surface region from n type to p type could be observed. The doped regions consisted of rastered small area pads. The Raman microprobe analysis was done in air using the $z(x,y)z$ configuration, with [001] the z axis and [100] the x axis. The 3 mW, 514 nm probe beam from an Ar$^+$ laser focused to 1.1 μm (full width at $1/e$) resulted in a temperature rise for the sampled spot of $\leqslant 50$ °C. Note that the $1/e$ probe length for Raman spectroscopy is half the absorption length, or ~ 540 Å at this wavelength.

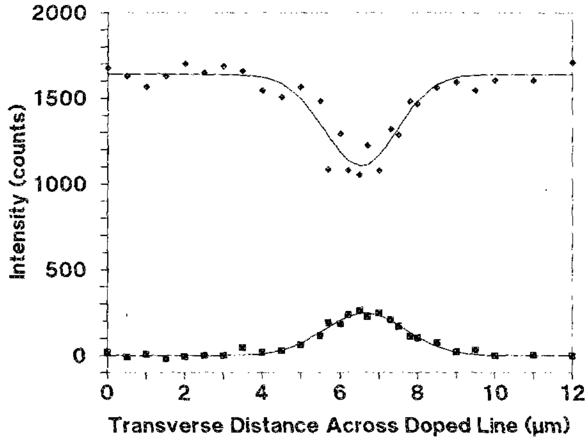

FIG. 3. TO and LO intensities measured at various distances across a laser-doped line. The solid lines are Gaussian fits to the data. LO intensity (◆) and TO intensity (■).

Comparison of the laser-doped sample and bulk p-type Zn-doped sample in Fig. 2(c) suggests that the surface is doped to a concentration of high $10^{18}/\mathrm{cm}^3$ to low $10^{19}/\mathrm{cm}^3$.[17] To investigate the lateral resolution of the laser-doping process, the intensities of the TO and LO peaks were measured as a function of position on a laser-doped $1\times10^{16}/\mathrm{cm}^3$ n-type sample. The results are shown in Fig. 3, where the TO and LO intensities were measured as the probe beam was moved in discrete steps along a line at 45° to the width of the doped line to improve lateral resolution. Using full width at $1/e$ values, the measured width from the TO trace (the wider of the two) is 3.1 μm. Removing the broadening of the trace due to the probe beam gives a width of 2.9 μm at 45°. Therefore, the width of the doped region at 90° is 2.0 μm, which is significantly narrower than the 2.9 μm wide processing beam, as has been reported previously.[3]

A more quantitative measure of the doping levels and depths was obtained through SIMS. In this case, Zn-doped substrates ($p = 5\times10^{16}/\mathrm{cm}^3$) were chosen to minimize charging effects associated with the use of negative oxygen ions for sputtering. The sensitivity of the SIMS machine to Zn atoms was determined to be in the low $10^{17}/\mathrm{cm}^3$ range through the use of implanted standards. Pads of 500×500 $\mu\mathrm{m}^2$ required for SIMS measurements were produced by rastering in 0.5 μm increments a 2.5–3.0 μm laser beam over the entire area at 25 μm/s. The SIMS measurements were done using a 200 nA oxygen primary ion beam at 15 keV scanned over a 0.25 mm^2 area at 6 s/frame. A scan gate of 30% was used to eliminate cratering effects.

Depth profiles obtained for several different temperatures within the process window for 25 μm/s scan speed and 0.01

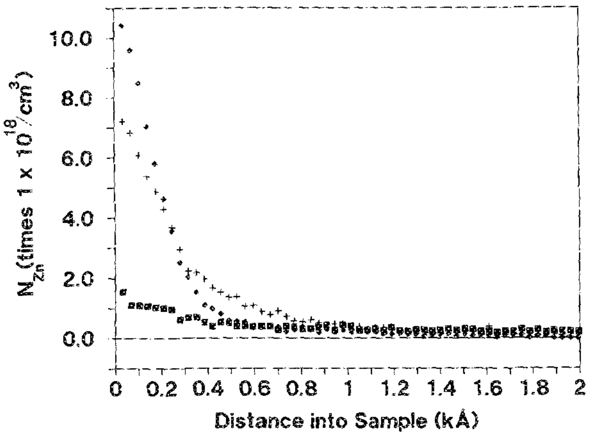

FIG. 4. SIMS measurements for three pads laser doped in a 10 mTorr DMZn ambient at a scan speed of 25 μm/s. Three different laser-induced temperatures were employed. T = 630 (■), 650 (+), and 670 (◆) °C.

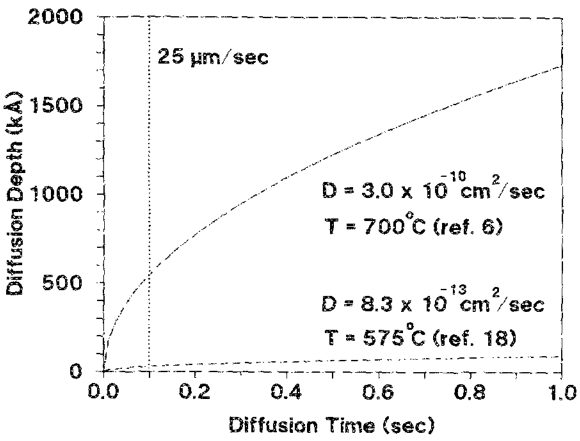

FIG. 5. Expected diffusion depths for various dwell times based on the results of Casey and Panish (Ref. 6) and Laidig *et al.* (Ref. 18). The vertical line shows the correspondence between stage speed and dwell time for a 2.5 μm wide processing beam.

Torr of DMZn are shown in Fig. 4. The results show that very shallow, relatively highly doped features could be obtained with our laser-doping process. Surface concentrations of up to 1×10^{19}/cm^3 were attained with depths $\leqslant$400 Å. Figure 5 shows expected diffusion depths for a Zn surface concentration of 3×10^{19}/cm^3 based on the data of Casey and Panish[6] and Laidig *et al.*[18] as a function of dwell time for two different temperatures bracketing those used in Fig. 4. The correspondence between the 25 μm/s stage speed and the laser dwell time for a 2.5 μm focused beam is denoted using a vertical line. Note that the measured diffusions obtained for the calculated temperatures chosen in Fig. 4 are consistent with those expected for the dwell time employed.

No attempt at determination of diffusion constants was made for these data since the shallow diffusions accomplished here are known to be complicated by the well known SIMS "tailing effect," where surface atoms are implanted into the substrate by the primary ions. Similarly, instrumental artifacts involving As concentrations near the surface obscure any As depletion that may accompany the laser doping process.

In a preliminary test for electrical activation, evaporated Al contacts were formed on n-type (1×10^{16}/cm^3) mesas laser doped under the same conditions of scan speed and DMZn pressure used in the SIMS and Raman experiments. The laser-induced temperatures ranged from 350 to 650 °C. It was found that the laser-doped diodes had consistently higher barrier heights and ideality factors than the control samples. The highest barrier height was elevated by 110 mV and had an ideality factor of 1.90. Further work to determine the response of these diodes to annealing through laser irradiation or conventional means is under way.

V. PROCESS WINDOW CONSIDERATIONS

It is well known that III–V compounds such as GaAs suffer depletion of the volatile component in the near-surface region upon prolonged exposure to typical doping temperatures in the range of ~650 °C and above unless special precautions involving capping layers or overpressures are taken. For the case of laser doping, such temperature-induced effects can only be exacerbated by the thermal stresses and strains resulting from the material's response to so localized a temperature. For example, both calculations[19] and experimental results[20] suggest that localized, high-temperature processing may induce dislocations at an irradiated surface for low scan speeds and high temperatures. Accordingly, the effects of moderate to intense 514 nm irradiation of GaAs samples in vacuum and in DMZn ambients were studied prior to the doping experiments to determine the boundaries of our process window in temperature, scan speed, and DMZn pressure.

Optical microscopy, SEM, stylus profilometry, and monitoring of the reflected 514 nm intensity during processing were used to characterize the nature and extent of surface damage. We found that exposure in vacuum to laser-induced temperatures $\leqslant$650 °C at typical scan speeds of 25 μm/s used for the doping experiments causes no observable changes in the irradiated surface. However, at low scan speeds of 1–2 μm/s with laser-induced temperatures$\geqslant$650 °C, noticeable changes in surface morphology did occur as evidenced by an uneven texturing of the surface. For laser-induced temperatures $\leqslant$530 °C, no changes in surface morphology were evident even for the longest dwell times investigated (3 min). The addition of a low-pressure DMZn ambient, such as used in our doping experiments, has no discernible effect at moderate incident intensities, which induce a temperature $\leqslant$650 °C, provided that short dwell times are employed. However, elevated DMZn pressures and high laser dwell times result in smooth etching of GaAs. Thus, at the lower boundary of the process window, the doping process is restricted by the need to prolong the dwell time at a given temperature for long enough to allow significant solid-state diffusion. On the other hand, the upper boundary of the process window is determined by the DMZn-related etching effect. These limitations in scan speeds, gas pressures, and laser-induced temperatures suggest that this technique is best suited for shallow diffusions of ~ 500 Å in depth.

CONCLUSIONS

A cw process for introducing *p*-type dopant into GaAs from an organometallic source has been developed. It has been shown that the process is capable of producing controlled, shallow diffusions to various concentrations, depending on the tempeature rise induced by the processing beam. In addition, a study of process window considerations for laser processing of GaAs has found that laser-induced temperature, laser dwell time, and ambient pressure must all be considered to establish a processing window for successful doping.

This single-step, maskless process allows the direct writing of narrow, shallow-doped features with real-time control over doping depth to be achieved through control of incident power and laser dwell time. Thus, smoothly contoured, laterally variable doping profiles can be generated for novel electron and optoelectronic devices.

However, the process suffers a significant drawback in the limited process window associated with cw laser treatment of bare GaAs in a DMZn ambient. Study of the DMZn-related etching process is under way to help reduce this effect and optimize the choice of future dopant source gases. Based on preliminary results, we believe the etching process is driven by the generation of reactive methyl radicals, which complex with the Ga and/or As atoms to yield volatile by-products. In this scenario, enhancement of the laser-doping process window can be achieved using parent molecules, which do not generate such by-products upon dissociation.

ACKNOWLEDGMENTS

The authors would like to thank R. Scarmozzino and D. Rossi for many valuable discussions. The work of T. Licata, D. Podlesnik, and R. Osgood was supported by Grant No. F49620-86-C-0067 from the Defense Advanced Research Projects Agency/Air Force Office of Scientific Research. The work of H. Tang and I. Herman was supported by Grant No. DAALO3-88-C-0009 from the Joint Services Electronics Program.

[1] H. Lezec, K. Ismail, L. Mahoney, M. Shepard, D. Antoniadis, and J. Melngailis, IEEE Electron Device Lett. **9**, 476 (1988).

[2] D. Ehrlich, R. Osgood, and T. Deutsch, Appl. Phys. Lett. **36**, 916 (1980).

[3] J. Tsao and D. Ehrlich, Mater. Res. Soc. Symp. Proc. **17**, 235 (1983).

[4] Y. Nissim, J. Gibbons, and R. Gold, IEEE Trans. Electron Devices **ED-28**, 607 (1981).

[5] Alfa Products (a division of Morton Thiokol Inc.), Danvers, MA (private communication).

[6] H. Casey and M. Panish, Trans. TMS-AIME **242**, 406 (1968).

[7] M. Lax, Appl. Phys. Lett. **33**, 786 (1978).

[8] A. Amith, I. Kudman, and E. Steigmeier, Phys. Rev. **138**, (4), A1270 (1965).

[9] J. McCaulley, V. McCrary, and V. Donnelly, J. Phys. Chem. **93**, 1148 (1989).

[10] *Thermophysical Properties of Matter*, The TPRC Data Series, edited by Y. S. Touloukian and D. P. Dewitt (Plenum, New York, 1972), Vol. 8, p. 679.

[11] *Thermophysical Properties of Matter*, The TPRC Data Series, edited by Y. S. Touloukian and D. P. Dewitt (Plenum, New York, 1972), Vol. 10, p. 462.

[12] E. D. Palik, in *Handbook of Optical Constants of Solids*, Academic Handbook Series, edited by E. D. Palik (Academic, New York, 1985), p. 438.

[13] T. Licata, D. Podlesnik, R. Colbeth, R. Osgood, and C. Chang, Amer. Inst. Phys. Conf. Proc. **167**, 250 (1988).

[14] G. Abstreiter, R. Trommer, M. Cardona, and A. Pinczuk, Solid State Commun. **30**, 703 (1979).

[15] G. Abstreiter, M. Cardona, and A. Pinczuk, in *Light Scattering in Solids IV*, Topics in Appl. Phys. **54**, edited by M. Cardona and G. Guntherodt (Springer, New York, 1984), p. 5.

[16] D. Olego and M. Cardona, Phys. Rev. B **24**, 7217 (1981).

[17] Note that the TO peak can also be observed in this configuration with the introduction of very high levels of *n*-type doping or nondoping elements in GaAs if sufficient disorder is induced in the lattice. This is not expected to be important here since both the Zn and C atoms available from DMZn are *p*-type dopants in GaAs, and laser-doped C was not detected using SIMS.

[18] W. Laidig, N. Holonyak, M. Camras, K. Hess, J. Coleman, P. Dapkus, and J. Bardeen, Appl. Phys. Lett. **38**, 776 (1981).

[19] L. Welsh, J. Tuchman, and I. Herman, J. Appl. Phys. **64**, 6274 (1988).

[20] J. Fletcher, J. Narayan, and D. Lowndes, in *Defects in Semiconductors*, edited by Narayan and Tan (North-Holland, Amsterdam, 1981), p. 421.